Correlation of scanning-tunneling-microscope image profiles and charge-density-wave amplitudes

B. Giambattista, A. Johnson, W. W. McNairy, C. G. Slough, and R. V. Coleman
Department of Physics, University of Virginia, Charlottesville, Virginia 22901
(Received 2 March 1988)

Scanning-tunneling-microscope (STM) studies of 4*Hb*-TaS_2 and 4*Hb*-$TaSe_2$ at 4.2 K show systematic correlation between the charge-density-wave (CDW) amplitude and the STM deflection. The 4*Hb* phases have both weak and strong CDW's in the trigonal prismatic and octahedral sandwiches, respectively. Scans on opposite faces of the same cleave allow a comparison of the STM response to the two types of CDW.

The transition-metal dichalcogenides exhibit a wide range of charge-density-wave (CDW) transitions[1] with different electron transfers, CDW superlattice wavelengths, and Fermi-surface modifications. In the constant-current mode the scanning tunneling microscope (STM) generates an image of the atomic arrangement at the surface by following the spatial modulation of the local density of states (LDOS) at the Fermi level at the position of the tunneling tip. The modulation of the conduction electron density at the wavelength of the CDW is easily detected by the STM in the constant-current mode and the amount of additional z deflection generated is related to the fraction of electrons transferred into the CDW condensate.

The 1*T* phases of TaS_2 and $TaSe_2$ have very strong CDW transitions with onsets above room temperature. Previous studies[2,3] with STM's operating at 77 and 4.2 K show images dominated by the $\sqrt{13}\mathbf{a}_0\times\sqrt{13}\mathbf{a}_0$ superlattice generated by the triple-q CDW. No modulation at the atomic wavelength has been detected at 77 or 4.2 K in 1*T*-$TaSe_2$ while a weak atomic modulation is observed in 1*T*-TaS_2. In addition the total z deflection ranges from 2.5 to 5.0 Å, far greater than expected for the normal spatial modulation of the conduction electron DOS.

By carefully studying a wide range of different phases with CDW's that involve widely different fractions of electron transfer into the CDW condensate we have been able to systematically compare the different z deflections generated by the CDW modulation. From these studies we can clearly associate the giant z deflection observed for strong CDW formation with the regions of charge deficit produced by the CDW and the accompanying minima in the LDOS of the conduction electrons above the surface. The minima cause the tunneling tip to make a close approach to the surface which can in turn further enhance the z deflection by mechanisms such as deformation of the surface by hard-core atomic potential repulsion as suggested by Soler *et al.*[4] In this paper we present STM images and corresponding profiles of the z deflections which clearly establish the relative roles of the CDW and atomic modulations. We also present the first complete set of STM images recorded from the 4*Hb* mixed phase crystals.

The 4*Hb* polytype has four three-atom layer sandwiches per unit cell and consists of alternating sandwiches of trigonal prismatic coordination and octahedral coordination. The electronic properties are, to a large extent, a composite of those observed in the pure octahedral (1*T*) phase and the pure trigonal prismatic (2*H*) phase. The crystals exhibit two independent CDW transitions which occur separately in the two types of sandwiches and are characterized by **q** vectors similar to those of the pure single coordination phases. Preliminary band-structure calculations[5] and some experimental observations suggest a small electron transfer between the alternating sandwiches. This can account for some modulations in the two CDW's, but they retain the characteristic structure found in the corresponding pure phases.

STM scans on both the octahedral and trigonal prismatic sandwiches show well-defined atomic modulations critical to a complete analysis of the contributions to the z deflection. The STM images for all of the different CDW structures have been recorded at similar values of tunneling current and bias voltage in order to minimize variations due to tunnel junction geometry, current flow and average tip-to-sample distance. The specific values are listed in the figure captions.

Crystals[6] of 4*Hb*-TaS_2 show the onset of a $\sqrt{13}\mathbf{a}_0\times\sqrt{13}\mathbf{a}_0$ CDW superlattice at 315 K in the 1*T* sandwiches and the onset of an incommensurate $\sim 3\mathbf{a}_0\times 3\mathbf{a}_0$ CDW superlattice at 22 K in the 1*H* sandwiches. Crystals[7] of 4*Hb*-$TaSe_2$ exhibit a CDW onset in the 1*T* sandwiches at 600 K which locks into a commensurate $\sqrt{13}\mathbf{a}_0\times\sqrt{13}\mathbf{a}_0$ superlattice at 410 K. The 1*H* sandwiches form a slightly incommensurate $3\mathbf{a}_0\times 3\mathbf{a}_0$ superlattice below 75 K.

STM scans of 4*Hb*-TaS_2 and 4*Hb*-$TaSe_2$ recorded from the 1*T* sandwich at 4.2 K are presented in Figs. 1 and 2 along with the profiles of z deflection generated along the line indicated in the scan image. The 1*T* scans from both 4*Hb* compounds show strong $\sqrt{13}\mathbf{a}_0\times\sqrt{13}\mathbf{a}_0$ superlattices of maxima and minima rotated 13.9° from the underlying atomic lattice. The profiles from both scans show very deep minima lying on a $\sqrt{13}\mathbf{a}_0\times\sqrt{13}\mathbf{a}_0$ superlattice and these minima account for the majority of the large z deflection of up to 2 Å. The CDW maxima contribute to the profile along with the superimposed atomic

modulation and an oscillating amplitude of ≤ 0.5 Å is observed at the upper level of the profile. We conclude that the atomic modulation of ≤ 0.5 Å arises mainly from the normal conduction electron modulation while the giant anomalous modulation is associated with minima of the CDW superlattice generated by CDW modifications of the LDOS.

The scans on the $1H$ sandwiches show a reduced total deflection of ≤ 1.0 Å and the profiles show the atomic modulation to be dominant. Figure 3 shows a comparison of the STM images obtained from the $1T$ and $1H$ faces of the same crystal cleave. The scan on the $1T$ face is shown in Fig. 3(a) and is dominated by the CDW maxima with a total z deflection of 2.6 ± 0.2 Å. The scan on the $1H$ face in Fig. 3(b) shows a total z deflection of ≤ 0.6 Å and a detailed profile is shown in Fig. 3(c). In addition to the atom pattern the scan on the $1H$ face shows a superimposed $\sqrt{13}\mathbf{a}_0 \times \sqrt{13}\mathbf{a}_0$ superlattice of weak amplitude which arises from the $1T$ sandwich ~ 6 Å below the $1H$ sandwich. This requires modulation of the conduction electron density in the $1H$ sandwich by the very strong CDW modulation in the $1T$ sandwich and this can enhance the STM z deflection observed for the $1H$ sandwich. In comparing Figs. 3(a) and 3(b) note that the $\sqrt{13}\mathbf{a}_0 \times \sqrt{13}\mathbf{a}_0$ superlattice patterns are mirror images of each other as expected for the two faces from the same cleave when mounted with the same basal plane

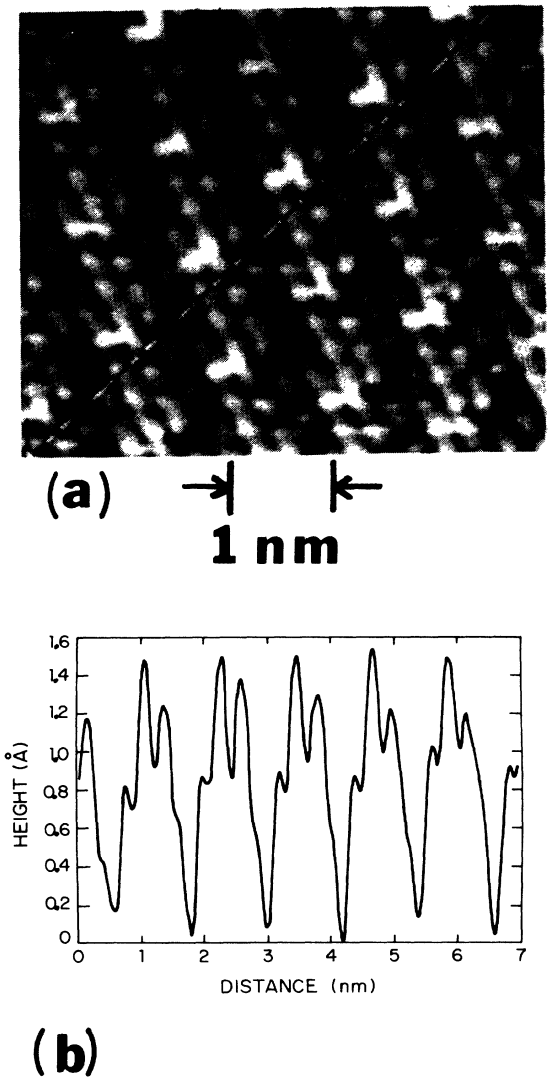

FIG. 1. (a) Grey scale image from the $1T$ sandwich of a $4Hb$-TaS_2 crystal at 4.2 K showing the CDW and atomic modulations ($I = 2.2$ nA, $V = 25$ mV, tip positive). (b) Profile of z deflection along the line shown in (a). Note the $\sqrt{13}\mathbf{a}_0 \times \sqrt{13}\mathbf{a}_0$ superlattice of deep minima.

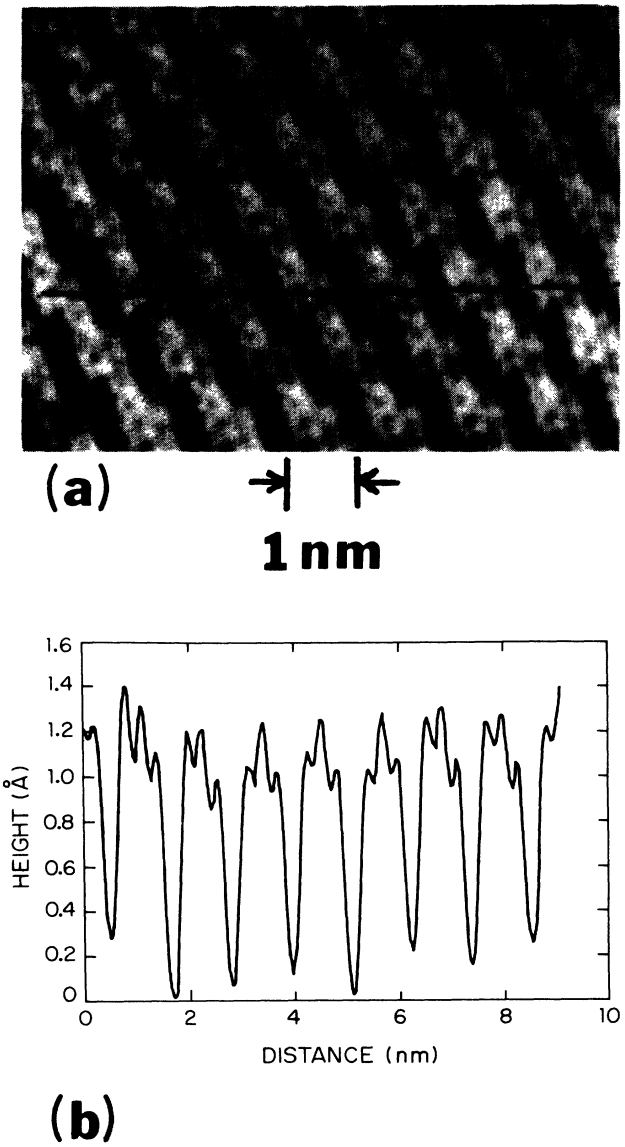

FIG. 2. (a) Grey scale image from the $1T$ sandwich of a $4Hb$-$TaSe_2$ crystal at 4.2 K showing the CDW and atomic modulations ($I = 2.2$ nA, $V = 25$ mV, tip positive). (b) Profile of z deflection along the line shown in (a). Note the $\sqrt{13}\mathbf{a}_0 \times \sqrt{13}\mathbf{a}_0$ superlattice of deep minima.

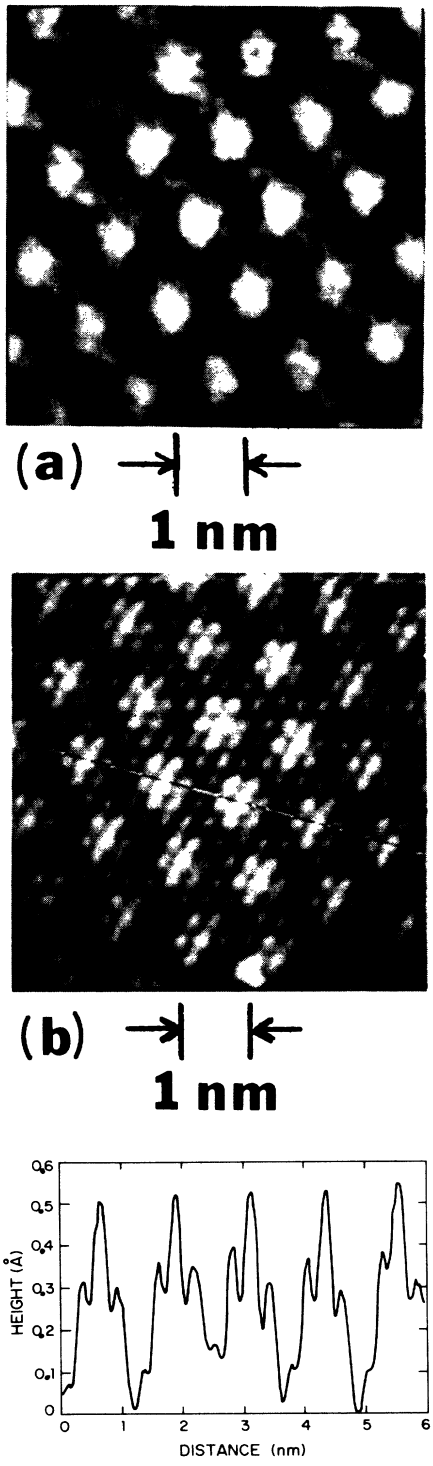

FIG. 3. STM images from opposite faces of a cleaved 4*Hb*-$TaSe_2$ crystal at 4.2 K ($I=2.2$ nA, $V=25$ mV, tip positive). (a) Grey scale image from the 1*T* face showing the dominant $\sqrt{13}\mathbf{a}_0\times\sqrt{13}\mathbf{a}_0$ CDW superlattice. (b) Grey scale image of the 1*H* face. Note the superlattice arising from the influence of the CDW in the 1*T* sandwich. (c) Profile of *z* deflection along the line shown in (b). Note the $\sqrt{13}a_0$ minima superimposed on the atomic modulation.

orientation. The $\sim 3\mathbf{a}_0\times 3\mathbf{a}_0$ CDW superlattice in the 1*H* sandwich itself is also present, but makes an extremely weak contribution to the STM scan. In selected scans a low-amplitude enhancement of $\lesssim 0.2$ Å can be detected with a wavelength of $3a_0$ as shown in Fig. 4(a). The $\sim 3\mathbf{a}_0\times 3\mathbf{a}_0$ superlattice is detected along with the $\sqrt{13}\mathbf{a}_0\times\sqrt{13}\mathbf{a}_0$ superlattice propagating from the 1*T* sandwich below. The two superlattices are rotated 13.9° from each other as clearly shown in the outlined hexagons at the lower right in Fig. 4(a). The two superlattices

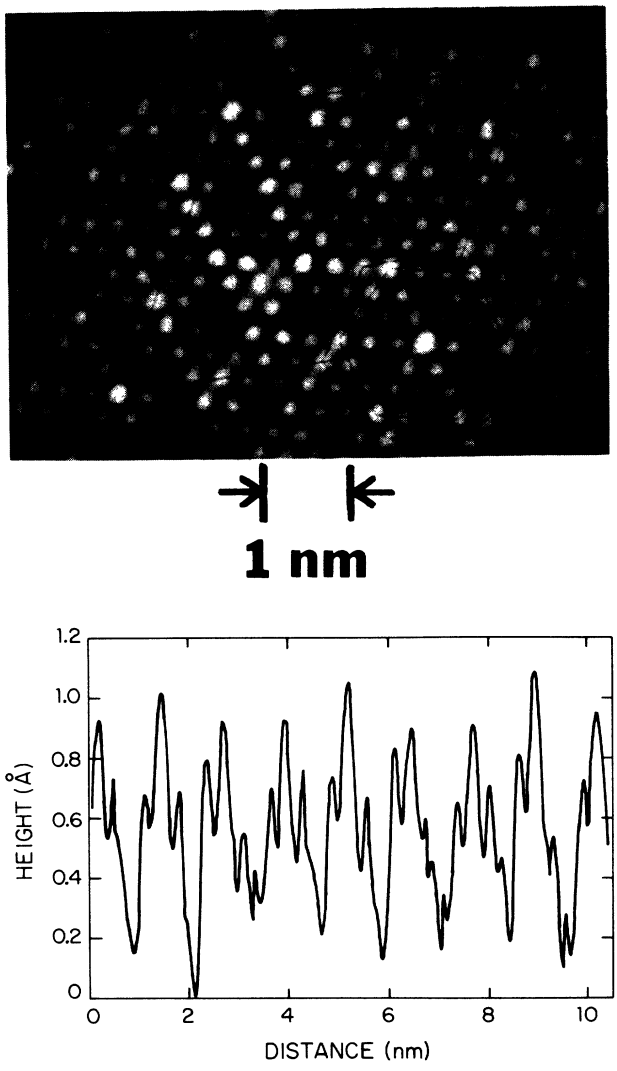

FIG. 4. (a) Grey scale image from the 1*H* sandwich of a 4*Hb*-$TaSe_2$ crystal at 4.2 K. Two hexagons outline the $3\mathbf{a}_0\times 3\mathbf{a}_0$ and $\sqrt{13}\mathbf{a}_0\times\sqrt{13}\mathbf{a}_0$ superlattices rotated 13.9° from each other. The rhombus outlines a unit cell of the $3\sqrt{13}\mathbf{a}_0\times 3\sqrt{13}\mathbf{a}_0$ super-superlattice which arises from the superposition of the $3a_0$ and $\sqrt{13}a_0$ modulations ($I=2.2$ nA, $V=25$ mV, tip positive). (b) Profile of *z* deflection along the edge of two adjacent $3\sqrt{13}a_0$ supercells. The three highest peaks each occur at an atom located at the corner of a $3\sqrt{13}a_0$ rhombus. These maxima are approximately 0.1 Å higher than the $\sqrt{13}a_0$ maxima.

combine to give a super-supercell of dimension $3\sqrt{13}\mathbf{a}_0 \times 3\sqrt{13}\mathbf{a}_0$ as outlined by the large rhombus. The profile extending over two supercells as shown in Fig. 4(b) clearly detects the extra 0.1 Å z deflection at a spacing of $3\sqrt{13}\,|\mathbf{a}_0| = 37.43$ Å (3.743 nm).

The above results on the $4Hb$ phases fit in consistently with the STM scans on the pure $1T$ and $2H$ phases which also support similar CDW superlattices. Examples for $2H$-$TaSe_2$ and $1T$-$TaSe_2$ measured at 4.2 K have been discussed in Ref. 3. The $2H$-$TaSe_2$ scans showed a relatively weak $3\mathbf{a}_0 \times 3\mathbf{a}_0$ CDW superlattice with a modulation of ~ 0.2 Å while the STM scans on the pure $1T$ phase crystals showed only the large-amplitude oscillations of 2–5 Å with the major deflection produced at the $\sqrt{13}a_0$ CDW superlattice wavelength.

The reduction in the conduction-electron LDOS generating the deep minima will depend on the exact details of the Fermi-surface modification and condensation of electrons into the CDW and can involve singularities in the LDOS as suggested by Tersoff.[8] The strength of such a CDW-induced singularity will depend on the amount of Fermi surface obliterated by the CDW and the strength of mixing between $\mathbf{k}_\parallel$ and $\mathbf{k}_\parallel + \mathbf{G}$. These effects will clearly be larger in the $1T$ phase and in the $1T$ sandwiches of the $4Hb$ phases. A hard-core potential repulsion with surface deformation can also contribute[4] when a strong minimum in the LDOS produces a close approach of the tip to the surface.

Although we do not know the absolute distance of the tip from the surface, the close approach at the CDW minima accounts for most of the anomalous z deflection observed and the atomic modulation when simultaneously present rides on the enhanced z deflection. The total absence of atomic modulation in pure $1T$-$TaSe_2$ at low temperature remains unexplained. However, the observation of a long-range modulation of the conduction electrons in the $1H$ sandwich of $4Hb$-$TaSe_2$ by the CDW in the $1T$ sandwich $\simeq 6$ Å away does suggest a very strong perturbation by this type of CDW. The observation of a long-range modulation is also consistent with the result of neutron-diffraction[7] experiments showing that the $1T$ CDW's in $4Hb$-$TaSe_2$ are phase correlated across the $1H$ sandwiches in the c direction while the $1H$ CDW's have random phases in the c direction suggesting only 2D long-range order in the basal plane for the $1H$ CDW's.

The authors thank P. K. Hansma and B. Drake for important contributions to the STM development. This research has been supported by the U.S. Department of Energy Grant No. DE-FG05-84ER45072.

[1]J. A. Wilson, F. J. Di Salvo, and S. Mahajan, Adv. Phys. **24**, 117 (1975).

[2]C. G. Slough, W. W. McNairy, R. V. Coleman, B. Drake, and P. K. Hansma, Phys. Rev. B **34**, 994 (1986).

[3]B. Giambattista, A. Johnson, R. V. Coleman, B. Drake, and P. K. Hansma, Phys. Rev. B **37**, 2741 (1988).

[4]J. M. Soler, A. M. Baro, N. Garcia, and H. Rohrer, Phys. Rev. Lett. **57**, 444 (1986).

[5]G. Wexler, A. Woolley, and N. Doran, Nuovo Cimento **38B**, 571 (1977).

[6]W. J. Wattamaniuk, J. P. Tidman, and R. F. Frindt, Phys. Rev. Lett. **35**, 62 (1975).

[7]F. J. Di Salvo, D. E. Moncton, J. A. Wilson, and S. Mahajan, Phys. Rev. B **14**, 1543 (1976).

[8]J. Tersoff, Phys. Rev. Lett. **57**, 440 (1986).

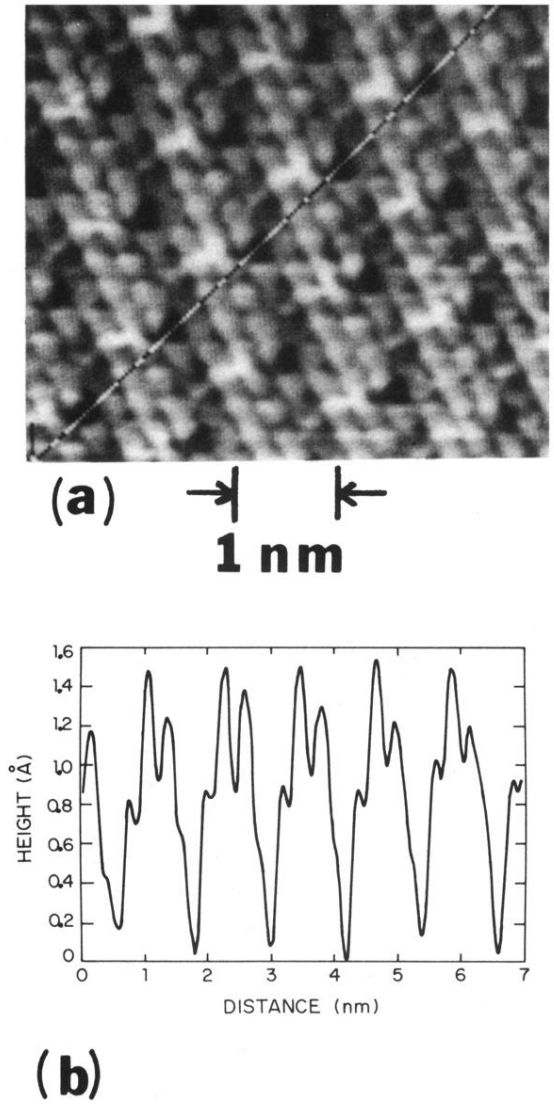

FIG. 1. (a) Grey scale image from the $1T$ sandwich of a $4Hb$-TaS_2 crystal at 4.2 K showing the CDW and atomic modulations ($I=2.2$ nA, $V=25$ mV, tip positive). (b) Profile of z deflection along the line shown in (a). Note the $\sqrt{13}\mathbf{a}_0\times\sqrt{13}\mathbf{a}_0$ superlattice of deep minima.

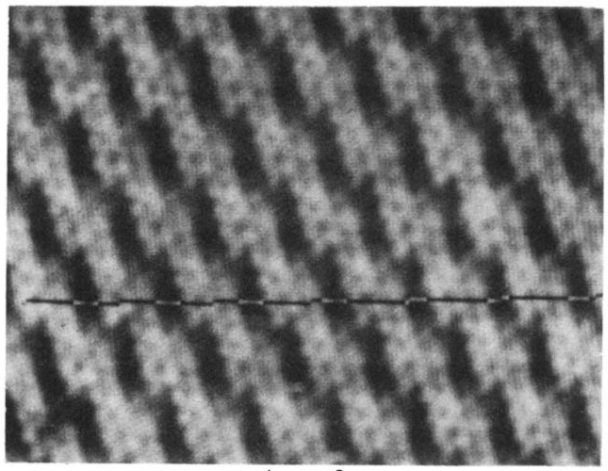

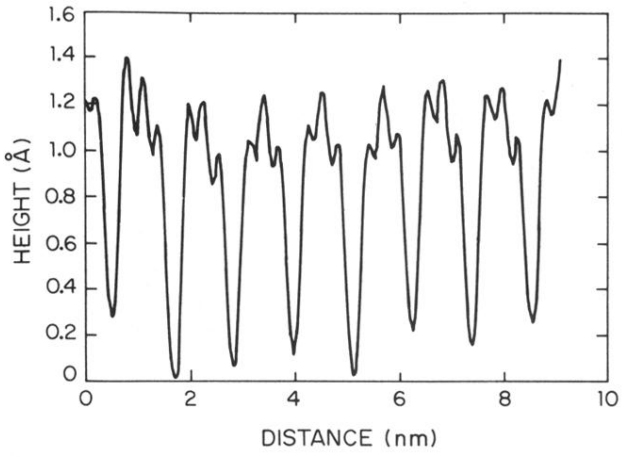

(b)

FIG. 2. (a) Grey scale image from the $1T$ sandwich of a $4Hb$-$TaSe_2$ crystal at 4.2 K showing the CDW and atomic modulations ($I=2.2$ nA, $V=25$ mV, tip positive). (b) Profile of z deflection along the line shown in (a). Note the $\sqrt{13}\mathbf{a}_0\times\sqrt{13}\mathbf{a}_0$ superlattice of deep minima.

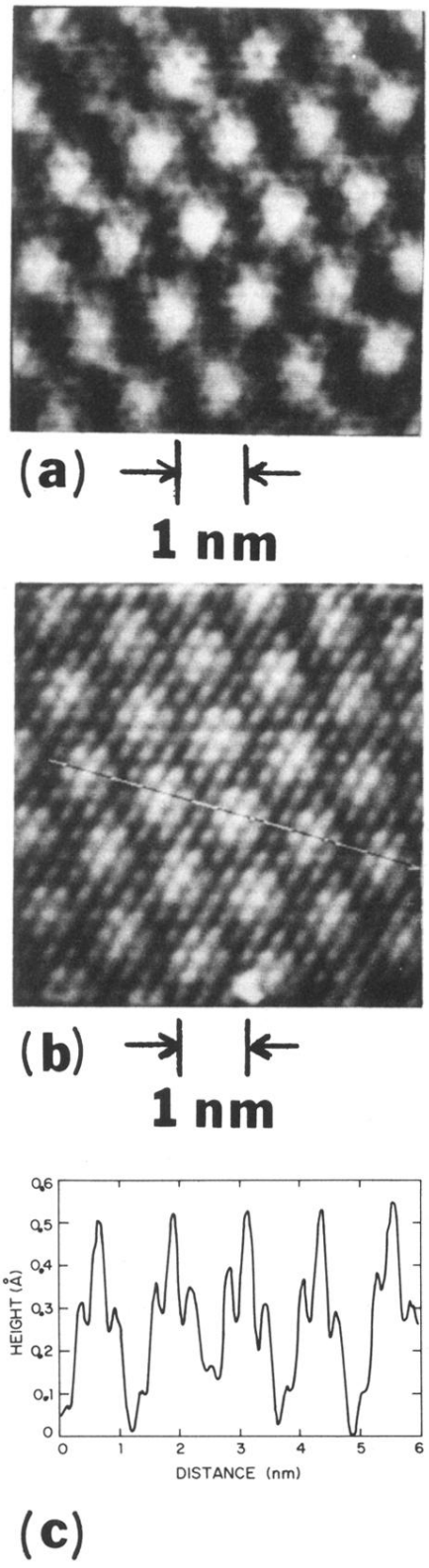

FIG. 3. STM images from opposite faces of a cleaved 4*Hb*-$TaSe_2$ crystal at 4.2 K ($I=2.2$ nA, $V=25$ mV, tip positive). (a) Grey scale image from the $1T$ face showing the dominant $\sqrt{13}\mathbf{a}_0\times\sqrt{13}\mathbf{a}_0$ CDW superlattice. (b) Grey scale image of the $1H$ face. Note the superlattice arising from the influence of the CDW in the $1T$ sandwich. (c) Profile of z deflection along the line shown in (b). Note the $\sqrt{13}a_0$ minima superimposed on the atomic modulation.

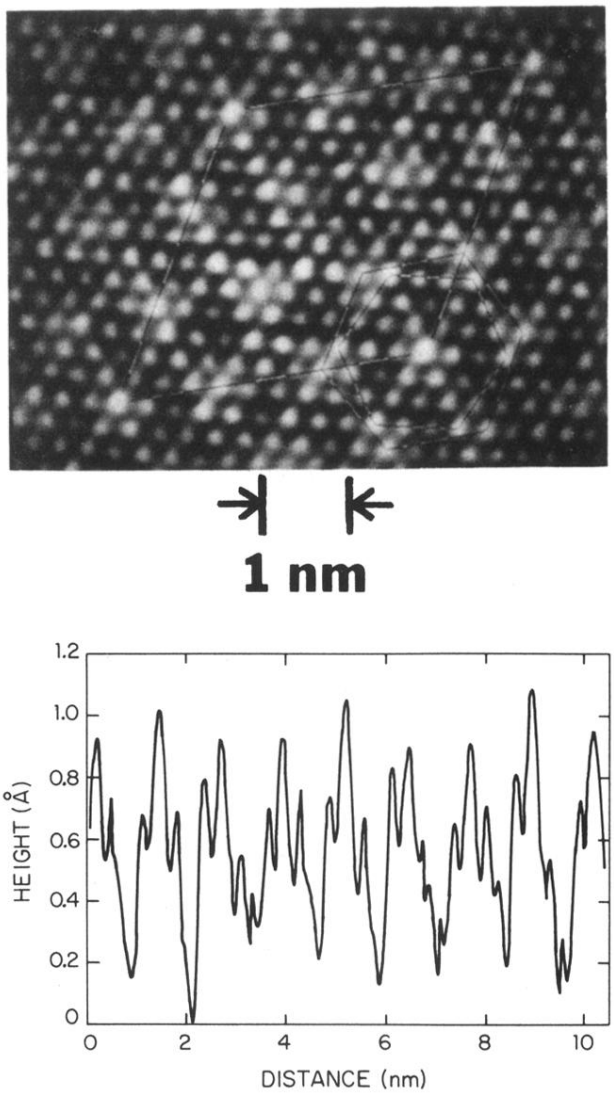

FIG. 4. (a) Grey scale image from the $1H$ sandwich of a $4Hb$-$TaSe_2$ crystal at 4.2 K. Two hexagons outline the $3\mathbf{a}_0 \times 3\mathbf{a}_0$ and $\sqrt{13}\mathbf{a}_0 \times \sqrt{13}\mathbf{a}_0$ superlattices rotated 13.9° from each other. The rhombus outlines a unit cell of the $3\sqrt{13}\mathbf{a}_0 \times 3\sqrt{13}a_0$ super-superlattice which arises from the superposition of the $3a_0$ and $\sqrt{13}a_0$ modulations ($I = 2.2$ nA, $V = 25$ mV, tip positive). (b) Profile of z deflection along the edge of two adjacent $3\sqrt{13}a_0$ supercells. The three highest peaks each occur at an atom located at the corner of a $3\sqrt{13}a_0$ rhombus. These maxima are approximately 0.1 Å higher than the $\sqrt{13}a_0$ maxima.